



Pulse width modulation-based TMS: Primary motor cortex responses compared to conventional monophasic stimuli

1. Introduction

Transcranial magnetic stimulation (TMS) is a non-invasive method of stimulating and modulating the nervous system. Most TMS devices are limited to predefined pulse shapes, such as monophasic or biphasic cosine-shaped pulses. Recently, the use of state-of-the-art power electronic instruments has permitted more control over the waveform parameters in several newer devices [1,2] (for a review of recent advances see supplementary file). A technique using pulse width modulation (PWM), called programmable TMS or pTMS, enables the approximation of a wide range of arbitrary pulses [3,4]. However, PWM-based pulses will introduce higher frequency harmonics, but our hypothesis is that cell dynamics will attenuate them.

The goal of this study is to use PWM to approximate conventional single-pulse monophasic TMS and assess the comparability of effects of both pulse forms on motor evoked potentials. The conventional monophasic pulse of a Magstim 200² stimulator was approximated by a custom-built PWM-based TMS device (pTMS2), making use of the modular device topology described in Ref. [4]. Computational modeling, resting motor thresholds (RMT), motor evoked potential (MEP) amplitude, latency and input-output (IO) curve measurements were compared within the same participants for both devices.

2. Materials and methods

TMS devices: We used a pTMS2 device that cascades two of the inverter cells introduced in Ref. [3] and generates magnetic pulses with five voltage levels, with no output filter. The conventional monophasic pulses were generated with a commercial Magstim 200² (Magstim Co., UK). Both devices were connected to the same 70 mm figure-of-eight coil (Magstim Co., P/N 9925–00). The simulated output pulses of the two devices are shown in Fig. 1(a) (and Fig. S4).

3. Physiological response models

To understand how the PWM stimuli interact with neural tissues, a computational model was applied before conducting the in-human study. This model also determined how many voltage levels are sufficient to approximate conventional TMS pulses with PWM-based pulses. The model, which integrates morphological neural models with transcranially induced electric fields [5], is used to compare the neural response to the Magstim and pTMS

pulses, similar to a previous study [6] (see supplementary file for more details). The temporal waveforms were simulated using MATLAB Simulink models adjusted to replicate the stimulation pulses of the devices used in the in-human study. The activation thresholds for PWM and conventional TMS pulses were calculated.

4. In-human study

Participants: The pTMS device and testing procedure were approved by the Central University Research Ethics Committee (CUREC), University of Oxford (R75180/RE002) to conduct this in-human study. Twelve healthy participants (mean age: 28.6 years, range: 22–37 years; 4 male) gave their informed consent to participate in the study. All participants were right-handed as assessed by the Edinburgh Handedness Inventory (Oldfield, 1971), had no current significant medical condition, and reported no other contraindications to TMS.

Procedure: Within each session, conventional and PWM stimuli were applied using the Magstim stimulator and pTMS devices, respectively, counterbalancing the order. The participants were seated in a chair with their arms resting on a pillow on top of a table in front of them. The coil was held by the operator, positioned over the left primary motor cortex and oriented at 45° to the midline with the handle pointing posteriorly. At the beginning of each session, the motor hotspot was determined with the Magstim stimulator, defined as the optimal scalp position where MEPs could be elicited in the right first dorsal interosseous (FDI) muscle. A Brain-sight neuronavigation system (Rogue Research Inc., Montreal, Canada) was used to track the position and orientation of the coil.

Electromyography (EMG) was recorded from the FDI of the right hand in a belly-tendon montage (for amplifier and filter details, see supplementary file). To find the motor-hotspot, the pulse timing and delivery was controlled by the experimenter using the foot pedal. Then, to confirm the hotspot, and to also find the RMT and the I–O curve, the pulses were applied automatically via scripts in Signal version 7.01 (Magstim device) and Control desk (pTMS2 device) software at varying inter-pulse intervals between 4.25 and 6 seconds.

To determine the RMT, 10 pulses were applied at each intensity and the EMG traces were inspected visually in real time. The stimulator outputs were adjusted manually to determine the minimum intensity required to evoke an MEP of ≥ 50 μ V peak-to-peak amplitude in 5 out of 10 consecutive trials.

For the IO curve, 15 MEPs at each intensity up to the maximum voltage achievable by the pTMS2 device were measured. Similar to other recent work [7], TMS stimuli were applied in increasing order

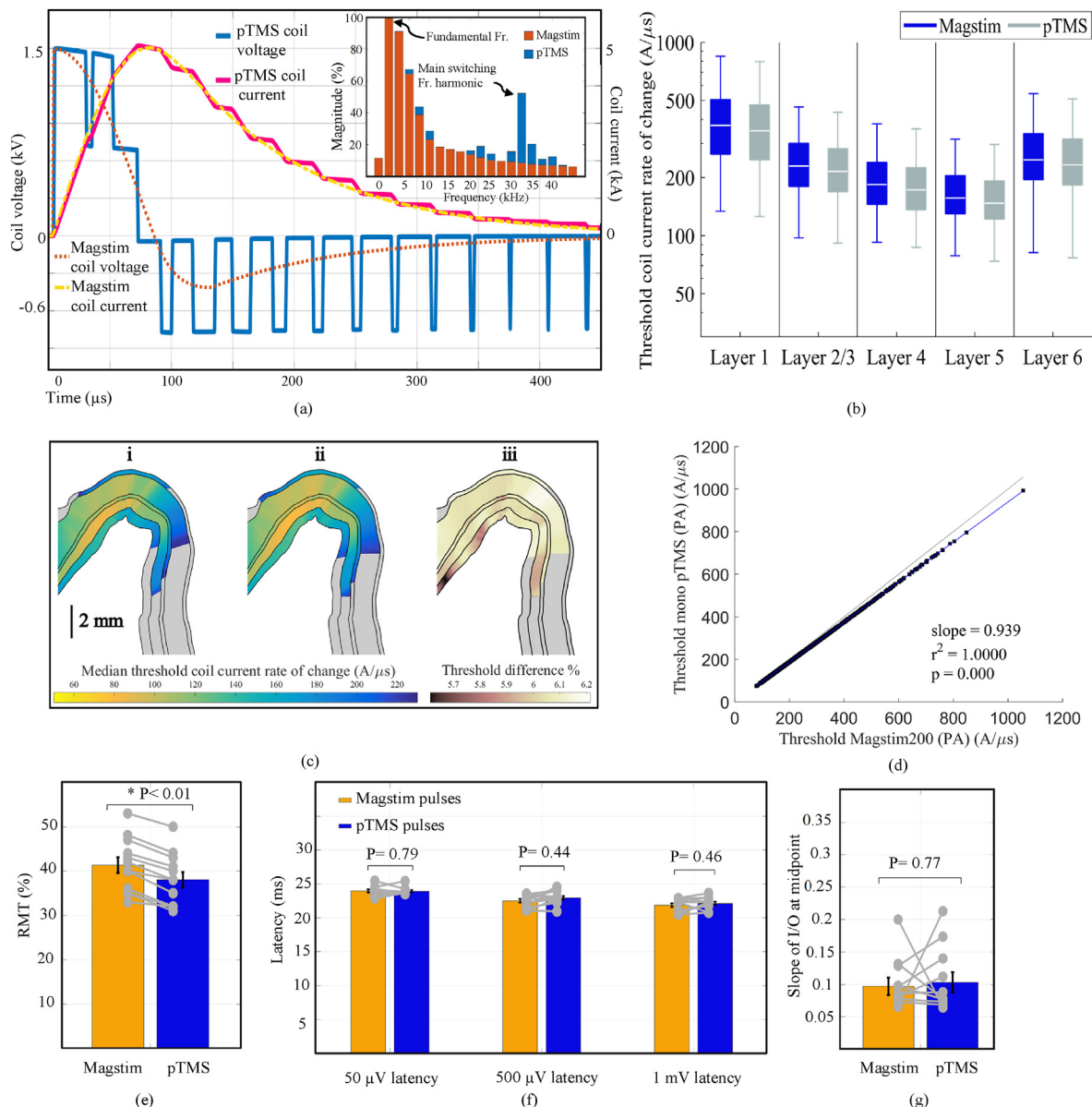


Fig. 1. Comparison of the Magstim 200² and pTMS2 system outputs and modeled responses for monophasic stimuli. (a) PWM coil voltage and current waveforms generated in the pTMS architecture in comparison with the Magstim waveforms. To approximate the monophasic pulse, the pTMS2 device synthesizes a staircase waveform using the PWM method. The voltage produced is a multi-step approximation of the target waveform. The frequency spectra of the Magstim and pTMS voltage waveform are also shown here. As expected, a PWM-equivalent pulse will have additional harmonic components. The largest harmonic is observed at 32 kHz (For more detail, see supplementary file) and is about 50% of the fundamental harmonic, while the high-frequency component corresponding to the Magstim pulse at the same frequency is 10%. The main switching frequency is 13 times higher than the main pulse frequency, and the dynamics of the neurons will attenuate them. It is important to note that the monophasic stimuli generated in conventional TMS devices, which are damped sinusoidal pulses, are not pure sine pulses and have high-frequency components. The y-axis represents a percentage of the fundamental frequency. (b) The modeled neural activation thresholds within the cortical area representing the hand muscle are shown in log scale, where blue represents the data from the Magstim 200² and grey from the pTMS2. Each boxplot includes the data from five clones within each layer with the outliers removed. (c) The median thresholds of the change in coil current for the six cortical layers are shown on a 2D cross-section of the crown of the pre-central gyrus for the pulse waveforms from (i) the Magstim 200² stimulator and (ii) the pTMS2 device. (iii) shows the modeled percent difference in median thresholds between the Magstim and pTMS pulses. (d) Correlation between the threshold coil current rate of change for the two pulses, with the linear regression displayed in blue and a line with a slope of 1 in grey for comparison. (e) Measured resting motor thresholds of the conventional monophasic pulse and its modulation equivalent generated by the pTMS device. To calibrate the MSO of the two devices, the positive peak coil voltage of the pTMS device was compared with the Magstim device. (f) Average MEP latencies were calculated for 50 μV, 500 μV and 1 mV peak-to-peak MEP amplitudes. While the MEP latencies varied with amplitude, they did not differ between the devices at any amplitude. (g) The slopes at the midpoints of the IO curves are shown for both pulse types. MEP measurements below 20 μV were set to 20 μV, as this was the lowest amplitude that was distinguishable from EMG signal noise. The MEP measurement was repeated 15 times for each amplitude, and the order of devices for the IO curves was counterbalanced to avoid order effects. For (e), (f) and (g), bars and whiskers show mean and standard error, respectively, with individual data points overlaid in grey. * indicates statistical significance. (For interpretation of the references to colour in this figure legend, the reader is referred to the Web version of this article.)

from low to high intensities in steps of 3% of the maximum stimulator output (MSO) of the Magstim 200. This fixed order of stimulation was chosen to compare the devices because the intensity of the pTMS2 device needs to be adjusted manually. The coil was lifted

from the participants' heads during the 1-min rest time between each set of stimuli.

Data analysis: For statistical analysis, we used repeated-measures ANOVA. The variables analyzed were: RMTs; input-

output curves; MEP latencies with peak-to-peak amplitudes of 50 μ V, 500 μ V and 1 mV, defined as the time point where rectified EMG signals surpass a mean plus two standard deviations of the 100 ms pre-stimulus EMG level [8]. The data were log-transformed, similar to Ref. [8], and a Gaussian-type least-squares curve regression with four parameters was utilized to fit the data points of each participant individually (see supplementary file).

5. Results and discussion

Physiological response models: Fig. 1(b) displays the thresholds for the neuron models in each layer within the cortical hand muscle representation as boxplots. The median excitation thresholds for both waveforms across a 2D cross-section of the pre-central crown is shown in Fig. 1(c). The models predict the activation thresholds to be 5.6–6.2% lower for the pTMS pulse than for the Magstim pulse. Linear regression between the thresholds for the two pulse types revealed a strong correlation ($r^2 = 1.000$, $p = 0.000$) with a slope of 0.939 (Fig. 1(d)), indicating a consistently lower threshold for the pTMS pulses.

MEP measurements: The RMTs, expressed as a percentage of the equivalent Magstim maximum stimulator output, were $41.34 \pm 6.07\%$ (mean \pm standard deviation) for the Magstim pulse and $38.00 \pm 5.91\%$ for pTMS stimuli (Fig. 1(e)). The pulse shape had a significant influence on the RMT ($F_{1,11} = 115$, $p < 0.01$). Notably, for all participants, the RMT for PWM pulses was (approximately 3%) lower than for the sinusoidal monophasic Magstim device pulses, a trend suggested by the modeling results. Using Cohen's d effect size, the difference between the RMTs was determined as a medium effect ($d = 0.53$). The difference in RMT may be related to the sharp edges and higher amplitude in the negative phase of the PWM pulses; another study has reported similar results for rectangular pulses [9].

The MEP latencies did not differ between devices; for 50 μ V MEPs: $F_{1,11} = 0.07$, $p = 0.79$, for 500 μ V: $F_{1,11} = 0.65$, $p = 0.44$, and for 1 mV: $F_{1,11} = 0.58$, $p = 0.46$, as shown in Fig. 1(f).

IO curves: It has previously been reported that the stimulus shape affects the slope of the IO curve at the midpoint [7,8]. Across the participants, the slopes of the IO curves did not differ between the devices ($F_{1,9} = 0.08$, $p = 0.77$), as displayed in Fig. 1(g).

Side effects: No adverse events occurred during or after the stimulations. After the experiment participants were asked to verbally report any differences they noticed between stimulation with the two devices. Participants did not report any subjective difference in experience, apart from a difference in the sound during pulse firing that was reported by all participants, which is most likely due to high frequency harmonics in PWM devices.

6. Limitations

PWM TMS pulses promise more flexibility in pulse generation but require further evaluation. The pTMS2 device is currently limited to lower stimulation amplitudes than the Magstim 200² for the pulse width used here, which precluded data collection from individuals with very high thresholds. The maximum pulse amplitude of pTMS2 was 1600 V, compared to the maximum outputs for the Magstim Rapid, MagVenture MagPro, and Magstim 200² which are approximately 1650, 1800 and 2800 V, respectively [9]. As the intensity of the pTMS2 device is adjusted manually, it is difficult to randomise stimulation intensities which may lead to hysteresis effects. To minimise this risk, stimuli were delivered in random intervals and participants had at least one-minute rest between each set of stimuli [10]. Additionally, measurements of the auditory signature are necessary for a future comparison of residual artifacts.

In summary, the measured motor responses suggest no difference in MEP latencies or IO curve slopes, but the RMT for PWM stimuli was approximately 3% lower across participants compared to the RMT for the Magstim device.

Data availability statement

The data and relevant scripts are available on the Open Science Framework (<https://osf.io/5ry92/>).

Prior presentation

An abstract related to this work was presented as a poster at the 4th International Brain Stimulation Conference.

Authorship contributions

MMS and KW contributed equally to this paper. MMS and TD designed and built the pTMS2 device. MMS and KW conceptualized the study, performed the statistical analysis, and drafted the manuscript. KW conceptualized and performed the modeling analysis. MMS, KW, JO conceptualized and performed the in-human study. JO and TD provided funding for the study. All authors revised and approved the final version of the manuscript.

Conflict of interest and financial disclosures

Prof. Denison reports personal fees from Medtronic and Bio-induction, outside the submitted work. Dr. Memarian and Ms Wendt report consulting fees from INBRAIN Neuroelectronics, outside the submitted work and Ms Wendt is funded by an MRC iCASE studentship with Magstim Company Ltd. Prof. O'Shea reports consulting fees from Welcony outside the submitted work. For the pTMS device, a patent application (GB2003206.6) was filed on 5th March 2020.

Declaration of competing interest

The authors declare that they have no known competing financial interests or personal relationships that could have appeared to influence the work reported in this paper.

Acknowledgements

This work was supported by a program grant from the MRC Brain Network Dynamics Unit at the University of Oxford (MRC MC_UU_0003/3), including an MRC iCASE studentship, and supplemental funding to TD by the Royal Academy of Engineering. JO'S is supported by a Sir Henry Dale Fellowship from the Royal Society and the Wellcome Trust (HQR01720). This research was conducted in part in the Wellcome Centre for Integrative Neuroimaging, which is supported by core funding from the Wellcome Trust (203139/Z/16/Z). For the purpose of Open Access, the authors have applied a CC BY public copyright licence to any Author Accepted Manuscript version arising from this submission.

The authors would like to thank Magstim Company Ltd (UK) for providing the stimulation coil and valuable guidance on device design considerations.

Appendix A. Supplementary data

Supplementary data to this article can be found online at <https://doi.org/10.1016/j.brs.2022.06.013>.

References

- [1] Zeng Z, et al. Modular multilevel TMS device with wide output range and ultrabrief pulse capability for sound reduction. *J Neural Eng* 2022;19(2).
- [2] Peterchev AV, D'Ostilio K, Rothwell JC, Murphy DL. Controllable pulse parameter transcranial magnetic stimulator with enhanced circuit topology and pulse shaping. *J Neural Eng* 2014;22(5).
- [3] Memarian Sorkhabi M, et al. Programmable transcranial magnetic stimulation– A modulation approach for the generation of controllable magnetic stimuli. *IEEE (Inst Electr Electron Eng) Trans Biomed Eng* 2020;68(6):1847–58.
- [4] Memarian Sorkhabi M, Denison T. A neurostimulator system for real, sham, and multi-target transcranial magnetic stimulation. *J Neural Eng* 2022;19(2).
- [5] Aberra AS, et al. Simulation of transcranial magnetic stimulation in head model with morphologically-realistic cortical neurons. *Brain Stimul* 2020;13(1):175–89.
- [6] Wendt K, et al. Comparison between the modelled response of primary motor cortex neurons to pulse-width modulated and conventional TMS stimuli. In: 43rd annual international conference of the IEEE engineering in medicine and biology society. EMBC; 2021.
- [7] Sommer M, et al. TMS of primary motor cortex with a biphasic pulse activates two independent sets of excitable neurones. *Brain Stimul* 2018;11(3):558–65.
- [8] D'Ostilio K, et al. Effect of coil orientation on strength–duration time constant and I-wave activation with controllable pulse parameter transcranial magnetic stimulation. *Clin Neurophysiol* 2016;127(1):675–83.
- [9] Goetz SM, et al. Enhancement of neuromodulation with novel pulse shapes generated by controllable pulse parameter transcranial magnetic stimulation. *Brain Stimul* 2016;9(1):39–47.
- [10] Pearce AJ, Ross AC, Dawson JK. A comparison of two methods in acquiring stimulus–response curves with transcranial magnetic stimulation. *Brain Stimul* 2013;6(3):306–9.

Majid Memarian Sorkhabi*

MRC Brain Network Dynamics Unit, Nuffield Department of Clinical Neurosciences, University of Oxford, Oxford, OX1 3TH, UK

Karen Wendt

MRC Brain Network Dynamics Unit, Nuffield Department of Clinical Neurosciences, University of Oxford, Oxford, OX1 3TH, UK

Department of Engineering Science, University of Oxford, Oxford, OX1 3PJ, UK

Jacinta O'Shea

Wellcome Centre for Integrative Neuroimaging (WIN), Oxford Centre for Human Brain Activity (OHBA), University of Oxford Department of Psychiatry, Warneford Hospital, Warneford Lane, Oxford, UK

Timothy Denison

MRC Brain Network Dynamics Unit, Nuffield Department of Clinical Neurosciences, University of Oxford, Oxford, OX1 3TH, UK

Department of Engineering Science, University of Oxford, Oxford, OX1 3PJ, UK

* Corresponding author. Institute of Biomedical Engineering, Old Road Campus Research Building, Oxford, OX3 7DQ, UK.
E-mail address: majid.memariansorkhabi@ndcn.ox.ac.uk (M. Memarian Sorkhabi).

4 December 2021

Available online 2 July 2022